Structure and Thermal Properties of New Comblike Polyamides: Helical Poly(β-L-aspartate)s Containing Linear Alkyl Side Chains

F. López-Carrasquero,[†,‡] S. Montserrat,[§] A. Martínez de Ilarduya,[†] and S. Muñoz-Guerra*,[†]

Departamento de Ingeniería Química, ETSIIB, Universidad Politécnica de Cataluña, Diagonal 647, E-08028 Barcelona, Spain, and Departamento de Máquinas y Motores Térmicos, ETSIIT, Universidad Politécnica de Cataluña, Colón 11, E-08222 Terrassa, Spain

Received January 27, 1995; Revised Manuscript Received May 6, 1995[⊗]

ABSTRACT: The structure and thermal properties of a series of novel comblike polyamides derived from nylon 3, poly(α-*n*-alkyl β-L-aspartate)s (*n* being the number of carbons in the linear alkyl side group) with $n = 6$, 8, 12, 18, and 22, were investigated. Polarizing infrared and solid-state ^{13}C CP-MAS NMR measurements revealed that these polyamides adopt α-helix-like conformations and that these structures are retained at high temperatures. Two first-order transitions at temperatures T_1 and T_2 separating three structurally distinct phases, namely, A, B, and C, were characterized for polymers with $n \geq 12$ by DSC and X-ray and electron diffraction methods. T_1 and T_2 ranged from −15 to +75 °C and from 50 to 129 °C, respectively, for *n* increasing from 12 to 22. Phase A ($T < T_1$) consisted of a layered structure of main chain helices with side chains crystallized in a separated hexagonal lattice. Phase B ($T_1 < T < T_2$) was found to be substantially like phase A but with side chains in the molten state. Phase C ($T > T_2$) was interpreted as a uniaxial arrangement of independent helices embedded in the amorphous side chain matrix. Microscope optical observations suggested that a cholesteric–nematic rearrangement is probably implied in the B–C transition. Members with $n = 6$ and 8 displayed a peculiar behavior. The octyl derivative crystallized by annealing in a three-dimensional structure composed of 13/4 helices of the type reported for poly(β-L-aspartate)s bearing short side chains while the uncrystallized polymer was arranged as in phase B. On the contrary, the hexyl derivative could neither crystallize nor organize in a layered structure. It was concluded from this study that the title compounds follow closely the general pattern of behavior described for poly(γ-*n*-alkyl α-L-glutamate)s, a family of thermotropic polypeptides that has received great attention in recent years.

Introduction

Poly(α-alkyl β-L-aspartate)s are nylon 3 derivatives with an alkoxycarbonyl group stereoregularly attached to every third backbone carbon atom of the repeating unit. These polymers are closely related to poly(γ-alkyl α-L-glutamate)s, a well-known class of synthetic polypeptides which, by analogy, can be regarded as deriving from nylon 2. In this nomenclature, α, β, and γ refer to the carbonyl position relative to the amino group in the corresponding parent amino acid. A schematic representation of the chemical formulas for the constitutional repeating units of these two families of polymers is given in Figure 1.

Studies carried out by our group a few years ago showed that poly(α-isobutyl β-L-aspartate) is able to crystallize in helical structures with features similar to the familiar α-helix of polypeptides and that the helical conformation is retained even in solution.[1–3] Certain properties related to the stiff helical nature of the macromolecule, such as formation of cholesteric liquid phases[4] and piezoelectricity,[5] were subsequently observed for this polyamide. Very recent studies made on other poly(α-alkyl β-L-aspartate)s including a variety of side chain compositions have shown that formation of helical structures seems to be a property common to the whole family of these compounds.[6–8] Among the different helical arrangements observed so far, the helix

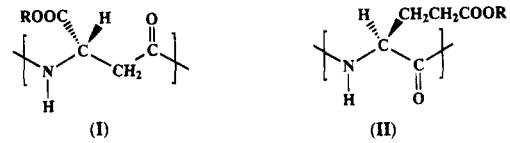

Figure 1. Chemical formulas for the structural units of the poly(α-alkyl β-L-aspartate)s (I) and poly(γ-alkyl α-L-glutamate)s (II).

containing 13 residues in 4 turns appears to be the conformation most frequently adopted. This consists of a right-handed helix with an axial repeat of ~2 nm and hydrogen bonds set between the amino group of the *i* residue and the carbonyl group of the $i + 3$ residue.[9] Although there is a close resemblance between this helix and the α-helix, the precise geometry of the molecule turns out to be noticeably different due to the opposite orientation assumed by the amido group with respect to the polarity of the main chain.[10]

α-Helical polypeptides bearing long paraffinic branches are remarkable because the rodlike character of the main chain is coupled with a flexible hydrophobic phase with which it is usually incompatible. There is a side chain critical length above which the supramolecular organization changes dramatically, giving rise to a series of unusual properties distinctive of the so-called comblike polymers.[11] These polymers attract great attention not only in their own in the study of supramolecular assemblies but also because they are promising materials for novel practical applications. Comblike poly(α-L-glutamate)s and poly(α-L-aspartate)s have been extensively investigated by several Japanese groups[12–14] during the past decade, and they continue to be an

* To whom all correspondence should be addressed.
† Departamento de Ingeniería Química, ETSIIB.
‡ Permanent address: Departamento de Química, Facultad de Ciencias, Universidad de Los Andes, Mérida 5101A, Venezuela.
§ Departamento de Máquinas y Motores Térmicos, ETSIIT.
⊗ Abstract published in *Advance ACS Abstracts,* July 1, 1995.

0024-9297/95/2228-5535$09.00/0

object of research nowadays.[15,16] In particular, Watanabe *et al.*[12] carried out a systematic examination of the structure and thermal properties of poly(α-L-glutamate)s with long linear alkyl side chains. These authors found that whereas the lower members of the family crystallize following the principle of optimum packing, higher homologs with alkyl groups containing ten or more carbons tend to adopt a biphasic layered structure and may generate thermotropic liquid crystals in a cholesteric or nematic arrangement. Such systems structurally resemble lyotropic mesophases with the flexible lateral chains in the molten state playing the role of the solvent. A critical review of these novel liquid crystalline polypeptides including their synthesis, characterization, and properties has been recently reported by Daly *et al.*[17]

In this work we are interested in poly(α-*n*-alkyl β-L-aspartate)s, i.e., poly(β-L-aspartate)s bearing linear alkyl side chains, abbreviated PAALA-*n*, where *n* represents the number of carbon atoms contained in the alkyl group. A general method of synthesis has been recently developed by us, which allows one to obtain these compounds for a wide range of *n* with a high degree of stereoregularity and large molecular weights.[18,19] While the structure of lower members of the series ($n \leq 4$) has been investigated in great detail as to conclude that they behave like poly(α-isobutyl β-L-aspartate),[7] no similar studies concerning members with side chains of medium or large size have been made to date. In the present study, a number of PAALA-*n* with *n* ranging from 6 to 22 have been examined by using a combination of techniques which include X-ray and electron diffraction, CP-MAS NMR, polarized infrared, and calorimetry measurements. The object is to evaluate the influence of the side chain length on the structure and thermal properties of these polymers and to know how they compare to poly(γ-*n*-alkyl α-L-glutamate)s with branches of similar sizes. Although an analogous pattern of behavior may be reasonably anticipated, certain differences between the two families will be expected from their dissimilarities in chemical structure. The additional methylene present in the main chain of poly(β-L-aspartate)s involves a less dense distribution of side chains in the space and will increase the flexibility of the main chain. Moreover, the mobility of the side chain will be more hindered than in poly(α-glutamate)s since the alkoxycarbonyl group is directly anchored to the polymer backbone.

Experimental Section

Materials. The five poly(α-*n*-alkyl β-L-aspartate)s used in this work were prepared by nonassisted anionic ring-opening polymerization of the corresponding optically pure (*S*)-4-(alkoxycarbonyl)-2-azetidinones. A detailed account of the synthesis of these polymers and their corresponding monomers has been published elsewhere.[8,20] The docosyl derivative ($n = 22$) was synthesized specifically for this work by applying the same method. Some data of these polymers relevant to this study are given in Table 1. Their molecular weights are in the range 200 000−450 000, they are soluble in chloroform, and they stand up well to temperatures above 200 °C. Poly(γ-*n*-octadecyl α-L-glutamate) was used in this work for comparative purposes and was prepared by Prof. K. Yoshioka (University of Tokyo) by transesterification of poly(γ-methyl α-L-glutamate) (M_v = 500 000) with stearyl alcohol. The content of this polymer in residual methyl ester groups is reported to be less than 5%.[22]

Measurements. Densities were measured by the flotation method in aqueous KBr solutions or methanol−water mixtures. For polarized infrared dichroism, films prepared by casting from chloroform were cut into strips and stretched under heating up to about 10 times their original length. Alternatively, orientation was accomplished with the polymer incorporated in a film of poly(ethylene oxide) (PEO) according to the method described by Ingwall *et al.*[23] A chloroform solution containing 2.5% (w/v) of PEO and 0.1% (w/v) of the polymer under investigation was evaporated to dryness and the resulting composite film stretched at room temperature. Infrared spectra were registered on a Perkin-Elmer 2000 FT-IR instrument equipped with a gold wire polarizer. To minimize errors due to the polarization monochromators, the orientation axis of the sample was placed at ±45° with respect to the direction of the entrance slit. Dichroic ratios ($\parallel/\perp$) of characteristic peaks were calculated from the absorbances measured for the parallel and perpendicular orientations of the sample to the infrared polarization vector.

Calorimetric measurements were performed with a Mettler TA-400 thermoanalyzer equipped with a low temperature range DSC-30 differential scanning calorimetric module at a heating rate of 10 °C/min under a nitrogen atmosphere and calibrated with indium standard. Samples weights of about 6 mg were used. Optical microscopy observations were made under a Nikon polarizing microscope provided with a Mettler FP-80 heating stage.

X-ray diffraction diagrams were obtained on flat films in a Statton-type camera using nickel-filtered copper radiation of wavelength 0.1542 nm and calibrated with molybdenum sulfide (d_{002} = 0.6147 nm). Polymer films prepared by casting from chloroform were placed with their surface either parallel or normal to the X-ray beam direction. Thermodiffractograms were recorded from unoriented films in a Siemens D-500 diffractometer with Cu Kα radiation provided with a TPK-A Park heating stage and a scintillation counter. For electron diffraction, films less than 50 nm thick were prepared by spreading a 1% chloroform solution onto a water surface. A Philips EM-301 instrument operating in the selected-area mode at 100 kV was used for this work.

Solid-state ^{13}C CP-MAS NMR spectra were recorded at 75.5 MHz in the temperature range −40 to +80 °C. A Bruker AMX-300 NMR instrument equipped with a CP-MAS accessory and a variable-temperature unit was used. Samples of 50−200 mg weight were spun at 3.9−4.2 kHz in a cylindrical ceramic rotor. All the spectra were acquired with contact and repetition times of 2 ms and 10 s, respectively, and 256 and 1024 transients were accumulated. The spectral width was 31.2 kHz, and the number of data points was 4K. Chemical shifts were externally calibrated against the higher field peak of adamantane appearing at 29.5 ppm relative to TMS.

Table 1. Data of Poly(α-*n*-alkyl β-L-aspartate)s Studied in This Work

R	M_0 (UCR)	$M_v \times 10^{-5}$ [b]	ϱ (g/mL)	T_d [c] (°C)
n-C_6H_{13}	199.28	2.1	1.07	307
n-C_8H_{17}	227.31	4.4	1.06[d]	341
n-$C_{12}H_{25}$	283.41	4.2	0.99	348
n-$C_{18}H_{37}$	367.57	2.0	1.03	330
n-$C_{22}H_{45}$[a]	423.39	~2	1.01	323

[a] Obtained by anionic polymerization of (*S*)-4-(docosoxycarbonyl)-2-azetidinone in dichloromethane with sodium pyrrolidone as initiator. [b] Estimated by viscosimetry by using the Mark−Houwink equation reported for poly(γ-benzyl α-L-glutamate).[21] [c] Peak maxima observed in the high-temperature region of DSC curves. [d] The same density is obtained whether the polymer is crystallized or not.

Results and Discussion

Transition Temperatures of PAALA-*n*. The DSC thermograms of PAALA-6 to PAALA-22 registered at heating are shown in Figure 2. To avoid traces overlapping, only the region between −50 and +200 °C has been represented except for PAALA-22, whose whole thermogram has been reproduced for illustration. As seen for PAALA-22, all traces exhibit a prominent peak above 300 °C corresponding to the melting−decomposi-

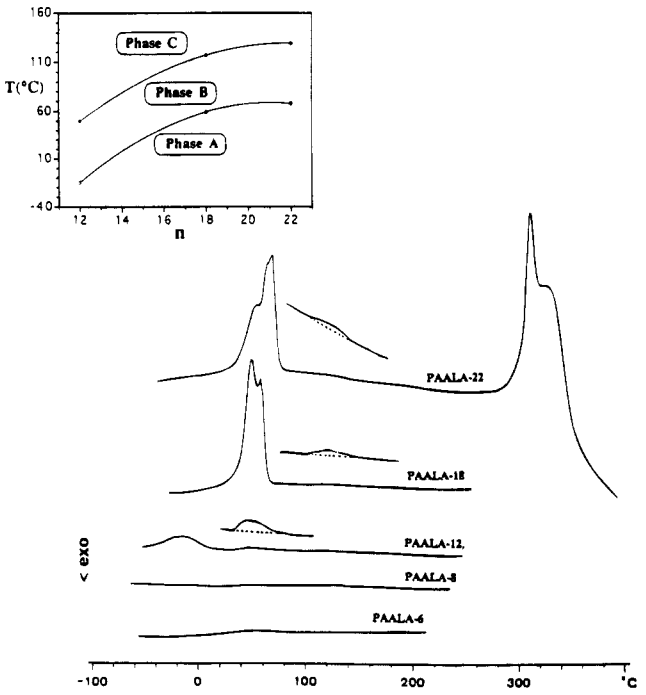

Figure 2. DSC thermograms of PAALA-n with T_2 peaks made apparent in enhanced traces. Inset: Temperature domains of phases A, B, and C in PAALA-12, -18, and -22 defined by their corresponding T_1 (○) and T_2 (●) temperatures.

Table 2. Calorimetric Data of Transitions in Poly(α-*n*-alkyl β-L-aspartate)s with $n \geq 12$

	transition A → B				transition B → C	
polymer	T_1[a] (°C)	ΔH_f (cal/mol)	ΔS_f[b] (cal/(mol K))	n_c[c]	T_2 (°C)	ΔH_f (cal/mol)
PAALA-12	−15	1172	4.5	1.9/2.8	50	130
PAALA-18	54−64	4850	14.4	7.9/8.8	117	100
PAALA-22	60−75	7290	20.9	11.9/12.8	129	110

[a] Two and three maxima are observed for PAALA-18 and PAALA-22, respectively. [b] Entropy changes approximately estimated by taking T_1 as the temperature of the highest peak. [c] Number of crystallized methylenes calculated by using enthalpic and entropic values of 650 cal/mol and 1.64 cal/(mol K), respectively.

tion of the polymer. This process is known to be common to the whole family of poly(β-L-aspartate)s and to take place along two successive steps involving intramolecular imidation and scission of the main chain, respectively.[8]

At temperatures below 200 °C, the thermal behavior of PAALA-n was found to be strongly dependent on the size of the side chain. Whereas no appreciable heat exchange was detected for PAALA-6 and -8, two endotherms at temperatures T_1 and T_2 ($T_1 < T_2$), the former much more intense than the latter, were observed in the traces of PAALA-n with $n \geq 12$. Both peaks tend to move toward higher temperatures as the length of the side chain increases. T_1 ranges from −15 °C for PAALA-12 to about 75 °C for PAALA-22, while the corresponding T_2 varies from 50 to 129 °C. The enthalpy associated with the endotherm at T_1 was found to increase with the side chain length and it ranges from 1.2 to 7.3 kcal/mol. In contrast, the amount of heat flux observed at T_2 is about 0.10−0.15 kcal/mol and its variation with composition is practically negligible.

The calorimetric data obtained from PAALA-n with $n \geq 12$ (Table 2) are highly comparable, in both temperatures and enthalpies, with those reported for poly(γ-n-alkyl α-L-glutamate)s with side chains of similar lengths.[12,22] By analogy with them, the thermal transition taking place at T_1 may be attributed to the fusion of the alkyl side chains leading to a partially disordered structure while the weak endotherm observed at T_2 could be related to a rearrangement of the structure generated at T_1. Accordingly, three phases, A, B, and C, with existence domains limited by the corresponding temperatures T_1 and T_2 will be distinguished in PAALA-n with $n \geq 12$, as diagrammatically represented in the inset of Figure 2. The fact that no paraffinic melting transitions are found for PAALA-8 and PAALA-6 is simply due to the insufficient length that the alkyl side chain has in these cases to crystallize by itself; this is in complete agreement with the thermal behavior reported for poly(α-L-glutamate)s[12] where a length of ten carbons is the minimum required to generate stable side chain crystals.

Structure of PAALA-*n* at Room Temperature. 1. X-ray Diffraction. Cast films of PAALA-n placed normal to the incident beam produced Debye−Scherrer patterns with similar features. They all consist of a more or less diffuse ring of spacing about 0.40−0.45 nm as well as an intense sharp ring of spacing ranging from 1.7 to 3.6 nm for n increasing from 6 to 22. When these films were diffracted in the edge-on position, oriented patterns consistent with a uniplanar orientation of the polymer were obtained for all cases except for PAALA-6. After stretching, all PAALA-n without exception produced fiber diffraction patterns revealing further differences among the polymers. Diagrams from stretched PAALA-18 and -22 display an equatorial row of reflections corresponding to successive orders of a basic spacing of 3.1 and 3.6 nm, respectively. In addition, an approximate hexagonal array of six intense spots with a spacing ~0.42 nm appears in the wide-angle region. Conversely, diagrams from stretched PAALA-6 to PAALA-12 merely consist of two intense arced-shaped reflections centered on the equator and near the meridian, respectively, which correspond to the two rings appearing in powder diagrams. Illustrative examples of each type of diagram are shown in Figure 3 for PAALA-18 and -12, and all the X-ray spacings observed at room temperature for every PAALA-n investigated in this work are compared in Table 3.

According to the model described for a variety of comblike polymers containing polymethylene side groups,[11,12,24] the X-ray scattering features displayed by PAALA-n with $n \geq 12$ can be interpreted in terms of a biphasic structure with main chains arranged side-by-side in layers and side chains segregated in a paraffinic phase filling the interlayer space. The reflections contained in the small-angle region of scattering are related to the spatial repeats associated with the layered structure. On the other hand, any orderly arrangement adopted by the paraffinic phase will become reflected in the pattern appearing in the wide-angle region. The discrete pattern of reflections displayed in the wide-angle region of diagrams of PAALA-18 and -22 demonstrates that side chains are crystallized in these two polymers whereas the diffuse scattering appearing instead in diagrams of PAALA-12 reveals that the paraffinic phase must be in a disordered state in this case. Provided that X-ray diagrams were registered at room temperature, these two versions of the biphasic model, i.e., with the paraffinic microphase crystallized or not, should correspond respectively to phases A and B defined above on the basis of calorimetric measurements.

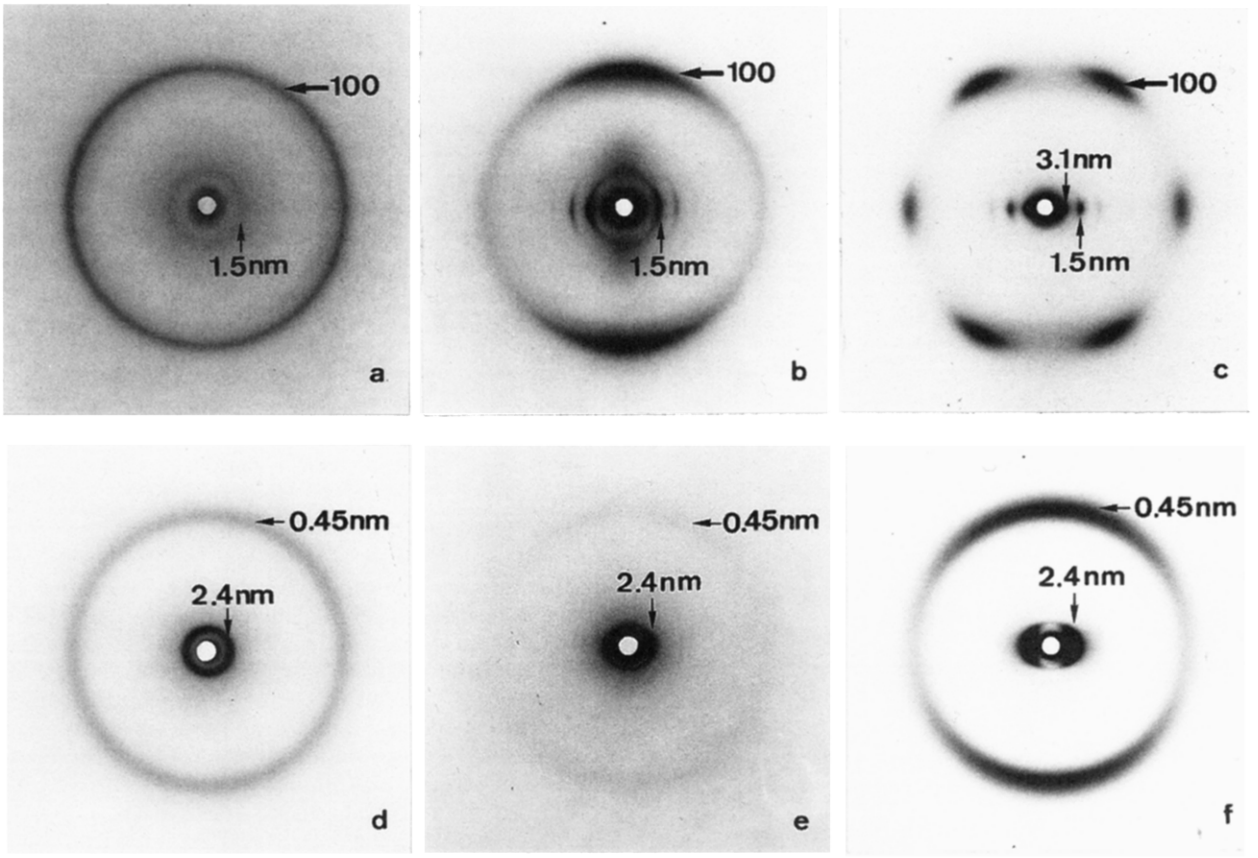

Figure 3. X-ray diffraction diagrams of films of PAALA-18 (a–c) and PAALA-12 (d–f) taken at room temperature. The polymer film was in a vertical plane. (a and d) Cast film viewed with the beam incident normal to the surface (transversal view). (b and e) Cast film viewed with the beam incident parallel to the surface (edge view). (c and f) Stretched film; the direction of stretching was vertical and the beam was normal to the surface. Sets of diagrams similar to a–c and d–f were recorded from PAALA-22 and PAALA-8, respectively. Only the most characteristic reflections are indicated on the pictures; a complete list of all the spacings recorded for the five PAALA-*n* is given in Table 3.

Table 3. Observed X-ray Spacings (nm) of Poly(α-*n*-alkyl β-L-aspartate)s at Room Temperature[a]

	PAALA-6	PAALA-8	PAALA-12	PAALA-18	PAALA-22
low-angle region	1.7 (vs)	1.8 (vs)	2.4 (vs)	3.10 (vs)	3.60 (vs)
				1.50 (m)	1.80 (s)
				1.04 (w)	1.19 (m)
				0.75 (vw)	0.86 (w)
					0.72 (vw)
wide-angle region[b]	0.45 (m, d)	0.45 (m, d)	0.45 (m, d)	0.46 (m, d)	0.45 (m, d)
				0.42–0.41 (vs), (100)	0.42–0.41 (vs), (100)
				0.24 (vw), (110)	0.25 (vw), (110)

[a] Visual estimates of intensities denoted as vs (very strong), s (strong), m (medium), w (weak), vw (very weak), and d (diffuse). [b] Indexing given for the paraffinic hexagonal lattice of $a_0 = 0.49$ nm.

With respect to the scattering observed in the small-angel region, it is noteworthy that only one Bragg spacing, which corresponds to the interlayer distance L_0, becomes defined on the equator of the diagram and no off-meridional reflections are seen in such a region. This means that the positional long-range ordering of the structure must be restricted along that direction normal to the layer plane; i.e., successive layers are irregularly sheared. Furthermore, the fact that higher orders of the L_0 basic spacing are brought out only when the polymer is in phase A (compare diagrams b and e in Figure 3) indicates that the regular stacking of the strata in such a phase is partially lost after the melting of the side chains.

The X-ray diffraction features displayed by PAALA-8 are quite similar to those displayed by PAALA-12 for both unoriented and oriented films. Therefore, the same type of structure may be reasonably assumed for both polymers at room temperature; i.e., the structure of PAALA-8 must be close to that of PAALA-12 in phase B. On the other hand, the X-ray results obtained from PAALA-6 evidence clearly that side chains are not ordered in this polymer, and in this respect it behaves similarly to PAALA-8 and -12. However, this PAALA differs from all others in that no uniplanar orientation is adopted by the polymer in cast films. Such a difference together with certain density considerations, which will be discussed in the appropriate section, suggest that PAALA-6 helices should not be arranged in layers but merely packed in a uniaxial structure with an average intermolecular distance L_0 of 1.7 nm.

2. Main Chain Conformation. X-ray diffraction data of PAALA-*n* with $n \geq 6$ are insufficient to ascertain the conformation assumed by the main chain in these polymers. Although the ~0.45 nm arced-shaped reflection appearing on the meridian of oriented diagrams might be attributed to the fourth layer line of a 13/4 helix of the type commonly found in poly(β-L-aspartate)s

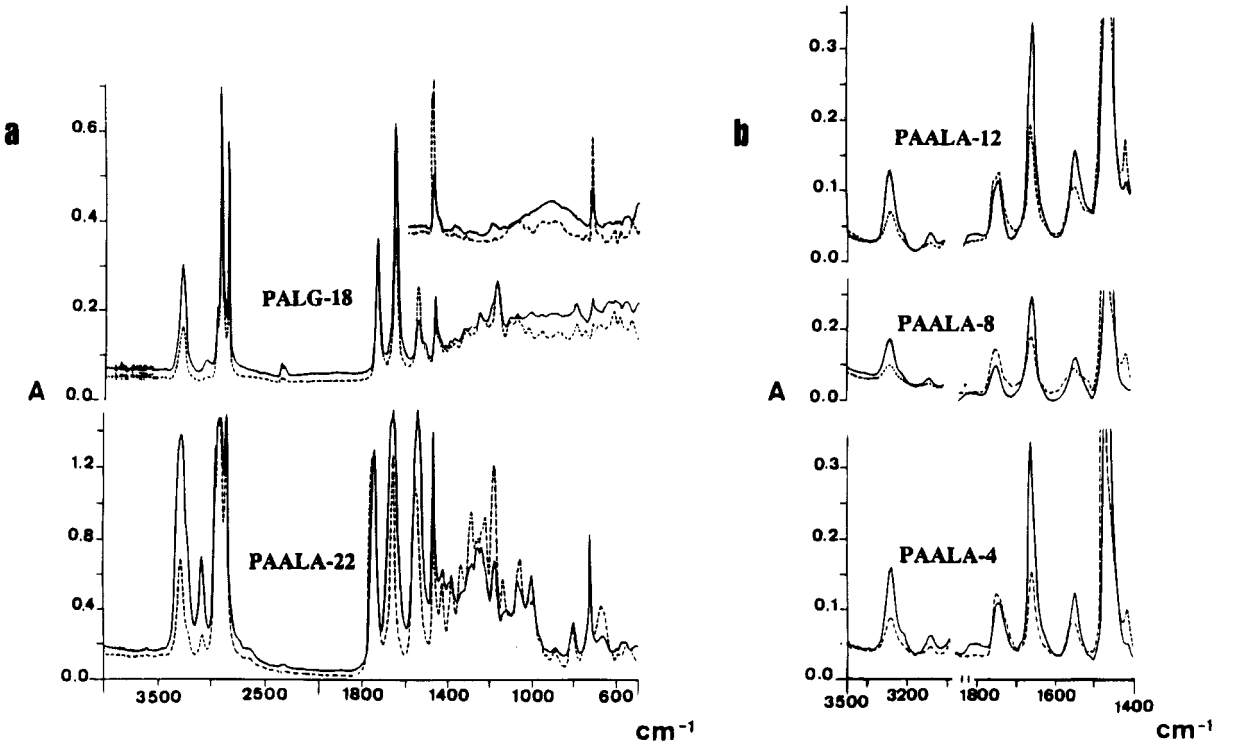

Figure 4. Infrared spectra of PAALA-*n* recorded with the polarization vector parallel (solid line) and perpendicular (broken line) to the orientation axis: (a) pure films; (b) polymer–PEO films. The spectra of poly(γ-*n*-octadecyl α-L-glutamate) (PALG-18) and PAALA-4 are included for comparison. Inset: Polarized spectra of oriented polyethylene in the 1600–600 cm^{-1} region.

Table 4. Polarized Infrared Spectral Data of Poly(α-*n*-alkyl β-L-aspartate)s

	band position (cm^{-1}) in parallel/perpendicular polarized spectra and their corresponding dichroic ratios, R (∥/⊥)							
polymer	amide A	amide I	amide II	C=O ester	$(CH_2)_n$	f_{min}[a]	S[b]	γ_0 (°)[c]
PAALA-4[d]	3287/3288	1656/1656	1543/1558	1748/1749		0.25		
	1.93	1.99	1.59	0.69				
PAALA-6	3285/3286	1654/1655	1542/1558	1741/1749		0.37		
	2.76	2.42	1.80	0.80				
PAALA-8	3285/3283	1655/1656	1543/1544	1743/1745		0.31		
	2.45	1.94	1.77	0.81				
PAALA-12	3282/3286	1655/1656	1541/1544	1740/1738		0.33		
	2.47	2.00	2.36	0.94				
PAALA-18	3287/3287	1654/1657	1541/1557	1741/1742	721/720	0.22	0.21	62
	1.87	1.17	1.15	0.94	1.27			
PAALA-22	3284/3285	1654/1656	1541/1557	1741/1742	721/721	0.26	0.24	63
	2.08	1.14	1.31	0.93	1.32			
PALG-18[e]	3287/3288	1654/1656	1550/1550	1738/1738	721/721	0.41	0.31	66
	2.03	1.68	0.49	1.05	1.45			

[a] Minimum orientation factor calculated on the basis of the dichroic ratio of the amide A band in PAALA-*n* and the amide II band in PALG-18. [b] Orientation parameter for the alkyl side chain. [c] Averaged angle of the side chain axis to the stretching axis. [d] Data taken from ref 10. [e] Poly(γ-*n*-octadecyl α-L-glutamate).

containing short side chains, lower order layer lines needed to characterize this conformation are here missing due to the lack of azimuthal order in the structure.

Polarized infrared spectroscopy has furnished strong evidence to infer that these polymers are arranged in a α-helix-like conformation close to that adopted by the lower members of the series. The infrared spectra of stretched films of PAALA-*n* recorded with the polarization vector parallel and perpendicular to the direction of stretching are shown in Figure 4. The spectra obtained under similar conditions from poly(α-*n*-butyl β-L-aspartate), which is known to be in the 13/4 helical conformation, and from the α-helical poly(γ-*n*-octadecyl α-L-glutamate) are included for comparison. Estimates of dichroic ratios for the characteristic absorption bands associated with the stretching modes of amide A (~3280 cm^{-1}, **OCNH**), amide I (~1650 cm^{-1}, **OCNH**), amide II (~1540 cm^{-1}, **OCNH**), and ester side group (~1740 cm^{-1}, **COO**) of the five PAALA-*n* under study and the reference compounds are listed in Table 4. A parallel dichroism demonstrative of an α-helix-like conformation is exhibited by both the amide A and amide I bands of all the polymers examined. The parallel dichroism exhibited by the amide II band of PAALA-*n* is known to be a feature characteristic of the 13/4 helix, which contrasts with the perpendicular dichroism that this band displays in α-helical polypeptides. A recent study combining infrared dichroism with modeling analysis has proved that such a discrepancy arises from the different inclination assumed by the amido group with respect to the chain axis in these two helices.[10]

3. Crystallized Side Chains. X-ray and DSC measurements have shown that the side chains of PAALA-18 and -22 in phase A are crystallized in an independent paraffinic microphase and that a similar structure is likely assumed by PAALA-12 at temperatures below −15 °C. The mode of packing adopted by the side chains within the crystallites, their orientation

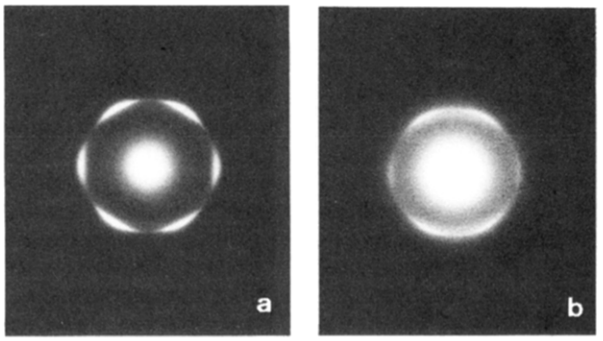

Figure 5. Electron diffraction diagrams recorded at room temperature from a film of PAALA-22 prepared by casting in chloroform: (a) "as prepared"; (b) after heating for a few minutes at 140 °C, which is above T_2. A similar set of diagrams was recorded for PAALA-18 when subjected to the same treatment.

with respect to the main chain, and the degree of ordering achieved in this phase are features which should be unraveled to attain a reasonable description of the structure of these systems.

The pattern appearing in the wide-angle region of the fiber X-ray diagrams of PAALA-18 and -22 (Figure 3c) suggests a hexagonal arrangement of side chains separated by a distance of 0.42 nm/sin 60° = 0.49 nm and extended normal to the main chain. Furthermore, the orientation of the pattern with respect to the stretching axis indicates that the hexagonal lattice is oriented with the 110 planes perpendicular to the main chain axis. The fact that the spots displaced at 60° from the equator appear with enhanced intensity should be logically expected from a partially randomized orientation of the whole structure around the stretching axis. Conversely, evenly intense hexagonal patterns with a basic spacing of 0.42 nm were obtained by selected-area electron diffraction of thin films of PAALA-18 and -22 (Figure 5a). Whereas no small-angle reflections are perceived in these diagrams, the 0.45 nm spacing attributable to the main chain is still observable. Such patterns indicate that these films are composed of large monocrystalline domains with the layered structure oriented parallel to the film surface and demonstrate definitely that side chains are crystallized in a hexagonal arrangement. It was noticed that the texture of these films remained essentially unaltered after they were subjected to heating above T_1 for a few minutes whereas the uniplanar orientation was partially lost when the films were heated above T_2 (Figure 5b). These observations are helpful in understanding certain optical effects exhibited by these films, which will be described below.

Infrared dichroism data have been used to estimate the inclination of the side chains respect to the main chain. A comparison of the dichroic ratios displayed by the characteristic bands arising from the alkyl side chains of PAALA-18 and -22 with those observed for the corresponding absorptions in stretched polyethylene reveals that the side chain methylenes display an opposite planar orientation (inset of Figure 4). Since the direction of the transition moment for the CH_2 rocking vibration is known to form an angle $\theta = 90°$ with the polymethylene chain axis, the averaged angle γ_0 formed by the side chains with the orientation axis was determined from the dichroic ratio R displayed by the 720 cm^{-1} peak. γ_0 is related to the orientation parameter S[11] by the expression

$$S = \frac{2 \sin^2 \gamma_0}{2 - 3 \sin^2 \gamma_0}$$

where S is equal to $1/R - 1$ for the particular case of $\theta = 90°$. The estimates of γ_0 resulting from these calculations for PAALA-18 and -22 as well as for PALG-18 used for comparison are shown in Table 4. They indicate that the orientation degree achieved by the side chains in poly(β-L-aspartate)s is practically the same as in poly(α-L-glutamate)s.[13] The minimum orientation factor f_{min} for the main chain was determined according to Fraser[25] by using the dichroic ratio of the amide A band, which is the band displaying maximum dichroism in the spectra. If both orientation parameters are taken into account, it may be concluded that the angle of the side chain to the main chain must be close to 90°.

The enthalpy associated with transition at T_1 may be used to estimate the fraction of methylenes participating in the paraffinic crystallite phase provided that data for various chain lengths are available.[26] Correlation of enthalpy against chain length across short ranges of n usually results in linear plots according to the equation

$$\Delta H_f = \Delta H_f(e) + nk$$

where $\Delta H_f(e)$ and k are constants reflecting the contribution made by the chain ends and each added methylene group to the heat of fusion. When ΔH_f obtained for PAALA-12 to PAALA-22 were plotted against n, a value of $n_0 \approx 10$ resulted for $\Delta H_f = 0$, which roughly represents the minimum length required for the methylene sequence to form a stable nucleus. The value falls within the range 9−12 usually encountered for comb polymers carrying paraffinic side chains[27] and turns out to be nearly identical to the critical length reported for poly(α-L-glutamate)s containing alkyl side chains of similar lengths.[12,22] Therefore, the approximate numbers of crystallized methylenes, n_c, in PAALA-12, -18, and -22 turn out to be around 2, 8, and 12 respectively (Table 2). Comparable results were obtained when entropies determined from the relation $\Delta S_f = \Delta H_f/T_f$ were used instead of enthalpies. It should be noted, however, that a larger error is likely implied in these calculations since the observed T_1 temperatures may be more or less far from the true equilibrium melting points.

The constant k gives the averaged enthalpy gain per mol of CH_2 and its value is known to be sensitive to the type of crystal lattice adopted by the alkyl side chains. The k value resulting for PAALA-n is about 650 cal/mol of CH_2, significantly lower than those found for the rhombic or triclinic to liquid transitions occurring in high n-alkanes and polyethylene, which are around 950 and 1000 cal/mol of CH_2 respectively.[27] The value is in better agreement with that reported for the fusion of the rather loose hexagonal crystal phase exhibited by n-alkanes at temperatures near their melting points.

Crystallization of PAALA-8. Among the PAALA-n containing long polymethylene side chains, PAALA-8 is unique in crystallizing by thermal treatment in a well-ordered three-dimensional structure. The X-ray diagrams obtained from this polymer before and after being heated at 108 °C for a few hours are shown in Figure 6. The general appearance of the pattern obtained from the annealed polymer is very similar to that of the patterns of n-butyl and isobutyl poly(β-L-aspartate)s crystallized in the hexagonal form.[2,7] Thus layer line intensities and positions appear to be consistent with a

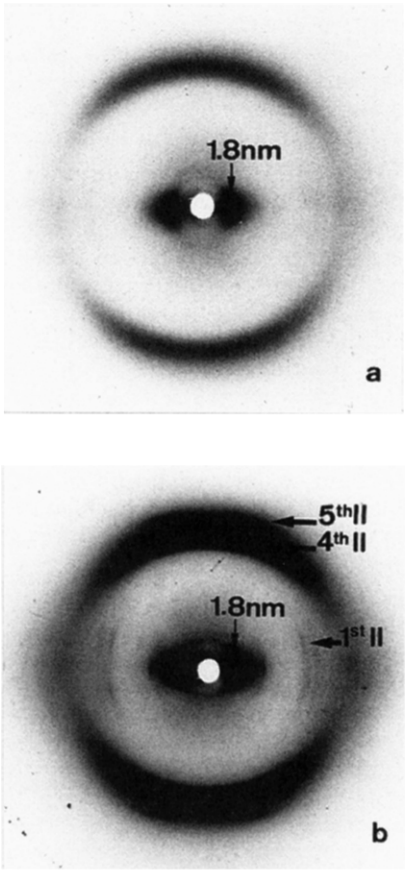

Figure 6. X-ray diffraction diagrams of stretched PAALA-8: (a) uncrystallized sample; (b) sample crystallized by annealing at 108 °C for a few hours. The stretching direction is vertical in both cases. The indexing of the crystallized pattern is given in Table 5.

13/4 helix of axial repeat c_0 = 1.99 nm. However, the equatorial reflections are not compatible with a hexagonal packing of helices but with a rectangular lattice of lateral parameters a_0 = 1.80 nm and b_0 = 1.23 nm. The whole pattern may be satisfactorily indexed on the basis of such a structure with good agreement between observed and calculated spacings (Table 5). The calculated density for this structure is 1.11 g/mL, in accordance with the observed experimental value of 1.06 g/mL, which is indeed the density observed for the uncrystallized polymer.

The fact that PAALA-8 can crystallize in a three-dimensional structure reminiscent of those adopted by short side chain containing PAALA-*n* is certainly striking and raises the question of how side chains may be efficiently arranged in such a structure. In this regard it is interesting to note that crystallization takes place without a perceivable change in density and that it results in an orthogonal array of helices with one of the lateral dimensions close to the L_0 interlayer distance observed for the uncrystallized polymer. In view of this, it is reasonable to interpret the crystal structure of PAALA-8 as comprised of sheets made of 13/4 helices with side chains occupying the intersheet space; sheets are separated 1.80 nm and the interchain distance within the sheets is 1.23 nm. A crude representation of what can be the mode of packing of the chains in this structure and how it compares with the common hexagonal packing of PAALA-*n* with $n \leq 4$ is given in Figure 7. A modeling analysis addressed to determine the precise conformation adopted by the side chain in the crystallized form of PAALA-8 is in progress.

Table 5. Observed and Calculated Spacings (nm) for Poly(α-*n*-octyl β-L-aspartate) Crystallized by Annealing

layer line	obsd spacings[a]	*hkl*[b]	calcd spacings[b]
$l = 0$			
	1.8 (vs)	100	1.800
	1.23 (s)	010	1.232
	1.03 (m)	110	1.017
	0.892 (w)	200	0.900
	0.466 (w, d)	400	0.450
	0.424 (w, d)	410, 320	0.423, 0.430
	0.407 (w)	030, 130	0.411, 0.410
	0.336 (w)	330	0.339
	0.306 (vw)	040, 140	0.308, 0.303
$l = 1$			
	1.075 (w)	011	1.048
	0.817 (w)	201	0.820
	0.600 (m)	021	0.588
	0.541 (m)	311	0.521
$l = 4$			
	0.491 (m)	004, 104	0.497, 0.480
	0.450 (vs)	114, 014	0.447, 0.461
$l = 5$			
	0.413 (w)	005	0.398
	0.394 (m)	105	0.386
$l = 8$			
	0.245 (w)	108	0.246
$l = 9$			
	0.229 (vw)	009, 109	0.221

[a] Visual estimates of intensities denoted as vs (very strong), s (strong), m (medium), w (weak), vw (very weak), and d (diffuse). [b] Indexing and spacings calculated for a rhombic lattice with parameters a_0 = 1.80 nm, b_0 = 1.23 nm, and c_0 = 1.99 nm.

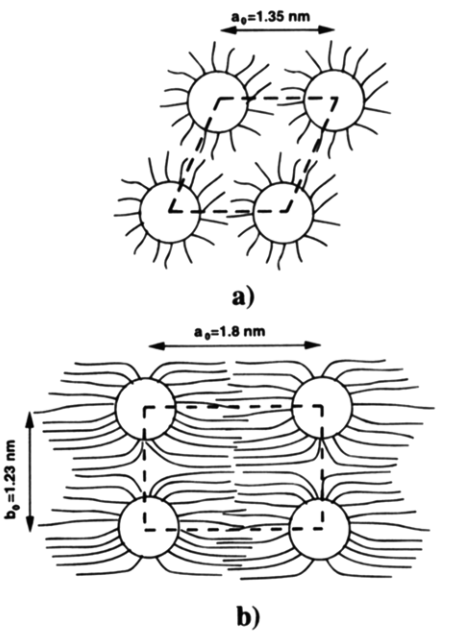

Figure 7. Approximate sketch of the cross-section of the hexagonal crystal form of PAALA-4 (a) and of the rhombic structure proposed for PAALA-8 in the crystallized state (b) illustrating the spatial distribution of the side chains in each case. The drawing is not scaled and it should be taken only for comparative purposes.

Structural Changes Associated with Thermal Transitions. 1. X-ray Diffraction as a Function of Temperature. To gain insight into the structural transformations lying under transitions T_1 and T_2, X-ray diffractograms from PAALA-12, -18, and -22 were recorded within temperature ranges including both transitions. The X-ray scattering profiles of PAALA-18 at temperatures increasing from 20 up to 165 °C are compared in Figure 8. Outstanding Bragg spacing variations in both the wide- and small-angle regions of scattering were observed for temperatures at which

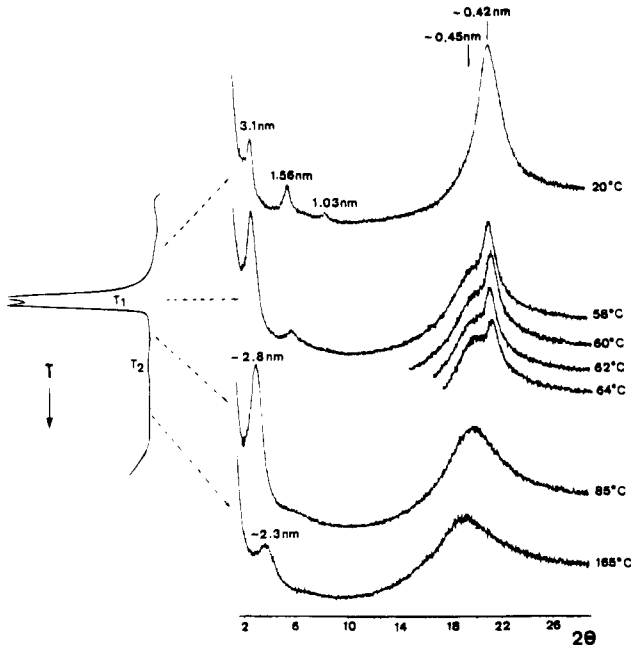

Figure 8. X-ray radial profiles of a PAALA-18 film taken at the labeled temperatures with indication of their positions relative to T_1 and T_2.

Table 6. Variations in the Main X-ray Spacings of Poly(α-*n*-alkyl β-L-aspartate)s with $n \geq 12$ by Effect of Temperature

	main X-ray spacings (nm) in the small-angle (SA) and wide-angle (WA) regions					
	PAALA-12		PAALA-18		PAALA-22	
phase	SA	WA	SA	WA	SA	WA
A	~2.5	0.42	3.1	0.42	3.6	0.42
B	~2.4	0.45	2.8	0.45	3.2	0.45
C	~2.3	0.45	2.3	0.45	2.5	0.45
Δ_{A-B}[a] (%)	~4		10		11	
Δ_{B-C}[a] (%)	~4		18		22	

[a] Percent decrease in the small-angle spacing observed at the indicated transitions.

transitions A−B and B−C take place. At temperatures below T_1, the diffractogram exhibited the 3.1 and 0.42 nm spacings characteristic of phase A. These spacings were replaced by 2.8 and 0.45 nm in phase B between temperatures T_1 and T_2. The small-angle spacing further reduced to 2.3 nm in phase C at temperatures above T_2 whereas almost no alteration was noticed in the wide-angle region. The reversed sequence of changes was observed at cooling. These results compare well with observations reported for PALG-18, where L_0 reduces from 3.2 to 2.5 nm when passing from phase A to phase C and where a value of 2.7 nm is observed at the intermediate phase B.[22] A similar pattern of behavior was found for PAALA-12 and PAALA-22 in their respective temperature intervals. The X-ray spacings characteristic of these polymers in the three phases are given in Table 6.

These observations are in agreement with the interpretation given above for transitions T_1 and T_2. The disappearance of discrete scattering in the wide-angle region clearly corresponds to the fusion of the paraffinic crystallites. However, the small contraction observed at L_0 indicates that molten side chains should remain in a nearly extended conformation. In contrast, a much larger contraction was found to accompany the transition occurring at T_2. Obviously, a profound rearrangement of side chains, presumably leading to a random conformation, must happen when the polymer passes from phase B to phase C. Accordingly, the decrease in L_0 observed at T_2 appears to be highly dependent upon the size of the side chain. Whereas a reduction in about 25% is found to take place for PAALA-22, the variation detected for PAALA-12 turns out to be only 4%.

2. ^{13}C NMR CP-MAS Measurements. Data presented above indicate that a certain rearrangement of the whole structure must happen at both T_1 and T_2. However, no evidence on the response given by the main chain to the thermal treatment is provided by these techniques, and very little is revealed about the conformation of the side chain in phases B and C. To address these questions, we have examined PAALA-*n* by ^{13}C NMR spectroscopy in the solid state as a function of temperature. It is well established that the chemical shifts of CH_2 in polymethylene chains are highly sensitive to both chain conformation and crystal structure and that chemical shifts of the backbone carbons in polypeptides may be used to distinguish between helical and nonhelical conformations.[28,29]

The spectra recorded from PAALA-*n* at 25 °C are shown in Figure 9. Assignments of peaks for the backbone carbons is straightforward on the basis of data available for poly(α-isobutyl β-L-aspartate)[30] as well as by comparison to their solution spectra.[8] Signals arising from the *n*-alkyl moiety are assigned by reference to NMR data reported for *n*-alkanes[28] and for the side chain of poly(γ-*n*-alkyl α-L-glutamate)s[29] and poly(β-*n*-octadecyl α-L-aspartate).[31] In Table 7, the chemical shifts observed for the PAALA-*n* at different temperatures are listed and compared with similar data reported on reference compounds. A close inspection of the data of PAALA-*n* contained in this table confirmed that all these polymers are in the helical conformation and that side chains in PAALA-18 and -22 are crystallized in a hexagonal lattice. The chemical shifts for the main chain carbons of every PAALA-*n* at 25 °C are very close to those observed for PAIBLA,[30] whose helical structure in the solid state was ascertained by X-ray analysis. On the other hand, a good correlation is found between the chemical shifts of the signals assigned to the alkyl side chain of PAALA-18 and PAALA-22 with those for *n*-alkanes crystallized in the hexagonal form, in particular when the positions of the methyl peaks are compared.

Figure 10 shows the ^{13}C CP-MAS NMR spectra of PAALA-22 registered within the temperature range 25−80 °C. No displacement of the chemical shifts of the backbone carbons was detected throughout the heat treatment, indicating that the helical conformation remains substantially unaltered. In contrast, significant changes were observed in the signals arising from the alkyl side chains, in agreement with the melting process taking place at T_1, which is around 70 °C in this polymer. In the proximity of 60 °C, the peak around 33.3 ppm ascribed to the interior methylenes crystallized in the all-*trans* conformation vanished, and a peak near 30.3 ppm attributable to the methylenes in fast equilibrium between *gauche* and *trans* conformations characteristic of the molten state emerged. At 80 °C, the replacement of the peaks was found to be practically complete. A similar evolution of the spectra with temperature was found for PAALA-18 and -12, with the most outstanding changes being observed at the corresponding T_1 temperatures. On the contrary, spectra from PAALA-6 and -8 remained unchanged within the examined range of temperatures, as expected from the

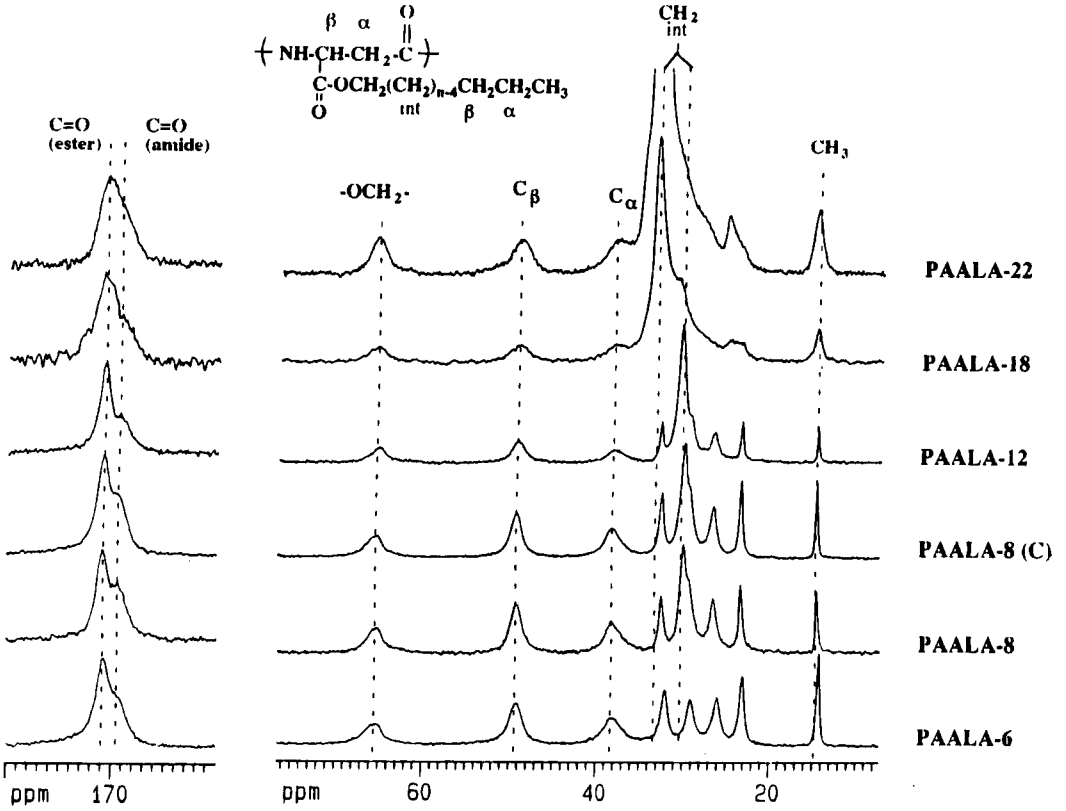

Figure 9. 75.5 MHz ^{13}C CP-MAS NMR spectra of PAALA-*n* registered at 25 °C. C_α and C_β refer to the main chain carbon atoms. Chemical shifts of signals arising from the main chain and the carboxylate group are similar for the whole series and correspond to the polymer in a helical conformation. Signals appearing below 35 ppm arise from the alkyl side chain which is crystallized in a separated phase in PAALA-18 and -22 and disordered in PAALA-12, -8, and -6. PAALA-8(C) refers to the polymer crystallized by annealing.

Table 7. 75.5 MHz CP-MAS ^{13}C NMR Chemical Shifts (ppm) of PAALA-*n* at Different Temperatures

		main chain and ester side group				alkyl side chain					
PAALA	*T* (°C)	C_α	C_β	CO_{amide}	CO_{ester}	CH_3	α-CH_2		β-CH_2	CH_2(interior)		OCH_2
PAALA-6	25	38.3	49.1	169.6	170.8	14.3	23.1		32.1	29.1	26.0	65.1
	80	38.0	49.2	sh	170.7	14.0	22.8		31.8	29.0	25.9	65.1
PAALA-8	25	38.4	49.2	169.4	170.9	14.6	23.3		32.5	30.0		65.2
	25[a]	38.3	49.2	169.7	170.9	14.6	23.3		32.5	29.9		65.1
	80	38.0	49.4	sh	170.8	14.2	23.0		32.2	29.6		65.0
PAALA-12	−40	37.9	49.3	sh	171.3	15.1		24.8	o		32.9	65.6
	25	38.1	49.2	169.3	170.9	14.6	23.4		32.7	30.5		65.0
	80	38.3	49.3	sh	170.8	14.2	23.0		32.4	30.1		64.9
PAALA-18	25	38.2	49.1	sh	171.0	14.8		24.8	o	30.9	33.3	65.4
	25[b]	38.2	49.3	sh	170.6	14.8	23.8		o	30.9	33.3	65.6
	40	38.0	49.4	sh	170.8	14.6	23.4		o	30.6	33.2	65.4
	60	38.2	49.5	sh	170.8	14.5	23.2		32.6	30.4		65.2
	80	38.1	49.5	sh	170.8	14.5	23.1		32.5	30.3		64.9
PAALA-22	25	37.7	48.9	sh	170.6	14.8		25.2	o		33.4	65.4
	25[b]	37.9	49.2	sh	170.7	14.8		25.1	o		33.3	65.3
	40	37.8	49.2	sh	170.5	14.8		25.1	o		33.3	65.2
	60	38.0	49.2	sh	170.7	14.7	23.2		o	30.4	33.3	65.1
	80	37.9	49.2	sh	170.7		23.1		32.5	30.3		64.9
PAIBLA[c]	25	38.7	49.7	sh	171.3							
PAALA-18[d]	25	36.7	49.7	171.4	173.1	14.1	22.8		32.0	29.8		65.4
n-alkanes[e]												
$C_{19}H_{40}$ (hexagonal)						14.8		25.0	34.9		33.7	
$C_{20}H_{42}$ (triclinic)						16.0		26.6	36.4		34.9	
$C_{23}H_{48}$ (rhombic)						15.1		25.6	35.1		33.6	
$C_{20}H_{42}$ (liquid)						14.1	22.6		31.9	29.7		

[a] Crystallized sample. [b] After heating at 80 °C. [c] Reference 30. [d] In $CDCl_3$–TFA.[8] [e] Reference 28. Abbreviations: sh, shoulder; o, neighboring peak overlapping.

disordered nature of the paraffinic phase in these two polymers. It is noteworthy that the same spectrum was obtained from PAALA-8 whether it was crystallized or not; this not only confirms that the 13/4 helix is present in both states but also indicates that the average conformation of the side chain must be rather similar. A detailed account of the variations detected in the chemical shifts of every PAALA-*n* with temperature is included in Table 7.

3. Optical Observations. The textures of phases A, B, and C and their dependence on temperature were examined under the polarizing optical microscope and

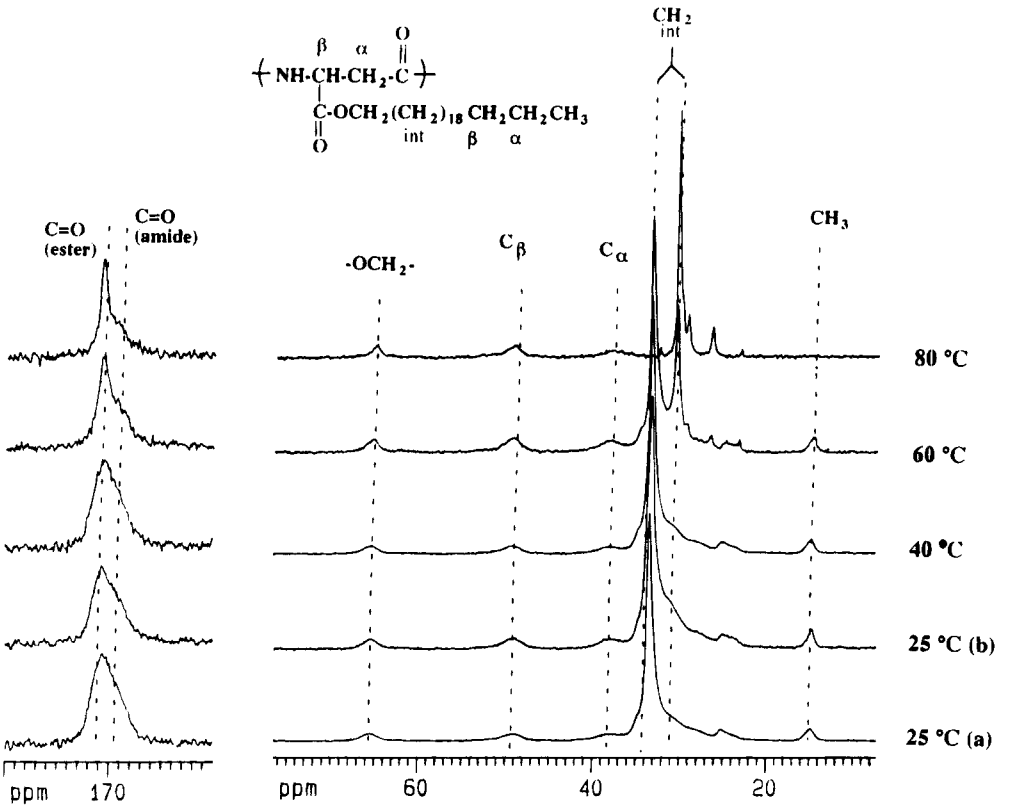

Figure 10. Evolution of the ^{13}C CP-MAS NMR spectrum of PAALA-22 as a function of temperature. The spectrum above 35 ppm is essentially unaffected by temperature whereas noticeable changes related to the melting of the side chains are observed in the high-field region. The spectra at 25 °C registered before (a) and after (b) the heating treatment are practically indistinguishable.

some preliminary conclusions could be drawn from these observations. Thin films of PAALA-12 prepared by casting appeared uniformly dark when observed through crossed polarizers at room temperature. This is the appearance that should be expected from a uniplanar arrangement of molecules lying in the plane of the film, in agreement with the structure revealed by both X-ray and electron diffraction for such type of film. After heating at temperatures below T_2, discrete birefringent zones of intense blue color appeared. Further heating above T_2 led to the complete disappearance of color and the film became homogeneously birefringent. On the other hand, striking beautiful colors changing from red to blue were displayed by oriented films of PAALA-12, -18, and -22 when subjected to heating at temperatures increasing from T_1 to T_2. At temperatures either below T_1 or above T_2, these films become uniformly white and display strong birefringency. The displayed sequence of colors was found to reverse upon cooling. The optical effects displayed by PAALA-n between temperatures T_1 and T_2 may be interpreted as owing to the selective reflection of circularly polarized light with a wavelength similar to the half pitch of the supramolecular helical structure present in phase B. In fact, preliminary circular dichroism measurements made on films in phase B showed ellipticity maxima in the 350−500 μm region, in agreement with what is expected from a cholesteric structure. On the other hand, the optical appearance exhibited above T_2 is consistent with a nematic structure oriented with the chains parallel to the film plane. All these observations should be taken just as indicative that a cholesteric−nematic transition may take place at T_2; obviously, more extensive and careful spectroscopic and microscopic observations are needed to characterize and understand completely the nature of such a transition.

An Overview of the Structure of PAALA-*n* and Their Phase Transitions. The results obtained in this work lead to the conclusion that PAALA-n with long side groups tend to be arranged with main chains and side chains occupying separated domains. Up to three structural phases differing in the manner in which such domains are organized are distinguished in PAALA-n with alkyl side chains containing 12 or more carbon atoms. The occurrence of different arrangements depending upon both temperature and side chain length is common among comblike polymers consisting of rodlike molecules with attached flexible chains. It is indeed the case for poly(α-L-glutamate)s containing long linear alkyl side chains.[12,17]

The L_0 spacings, which correspond to the interlayer distance for PAALA-8 to PAALA-22 and to the interchain distance for PAALA-6, observed for the five polymers under study are plotted against n in Figure 11. The a_0 and 100 spacings of the hexagonal lattices in which the poly(β-L-aspartate)s bearing alkyl side chains with n = 1, 2, and 4 are known to crystallize[8] are also represented for comparison. As logically expected, L_0 tends to increase with the length of the alkyl group at any temperature and whichever rank of side chain size is concerned. For PAALA-n with $n \geq 12$, the spacings corresponding to phases A and B may be fitted in two respective straight lines which tend to converge at $n \approx 10$. This makes sense since about ten side chain methylenes remain disordered in phase A. The increment of L_0 per carbon atom in phase A is approximately 0.12 nm, which is the value predicted for a polymethylene chain crystallized in the *all-trans* conformation. The slope of the line corresponding to phase B is 0.10 nm/carbon atom, indicating that side chains in this phase must be substantially extended in spite of being in a disordered state. Although L_0 for PAALA-6 seems

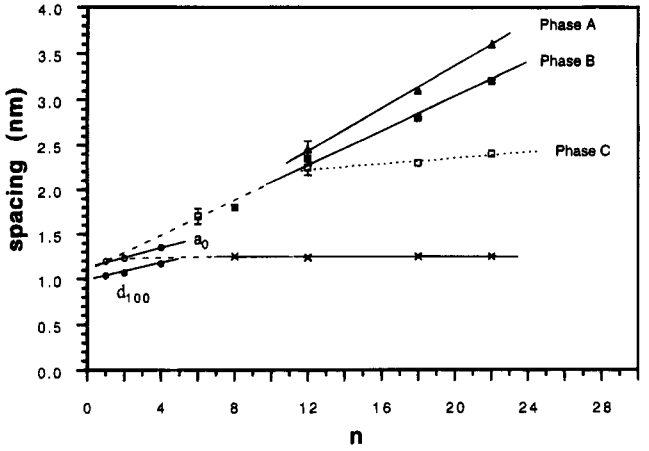

Figure 11. X-ray spacings in PAALA-n as a function of the number of carbons contained in the alkyl side chain for different temperatures: (▲,■) L_0 in phases A and B, respectively; (□) L_0 in phase C; (×) interchain distance within the layers in phase A calculated from L_0 and experimental densities; the value taken for PAALA-8 is the b_0 parameter of the rhombic lattice determined for the crystallized form (see text); (○,●) a_0 and 100 interplanar spacings in PAALA-n with $n \leq 4$ taken from ref 7.

to follow the trend observed for phase B, the X-ray results obtained from this polymer did not reveal any type of structural arrangement other than a loose side-by-side packing of helices. The decrease of L_0 with n in phase C is very slight, which is consistent with a random conformation of side chains. On the other side, the increment of a_0 observed in short side chain containing PAALA-n is also small, about 0.06 nm per alkyl carbon atom, as might be expected from alkyl chains being in a twisted conformation. It is noteworthy that phase B and a_0 lines tend to converge at a spacing near 1.15 nm for $n = 0$. Such spacing may be envisaged as the distance separating the layers in poly(β-L-aspartate)s in which the alkyl group has been removed.

L_0 for uncrystallized PAALA-8 was found to correlate fairly well with the line drawn for phase B. This is consistent with the diffracting similarities found between uncrystallized PAALA-8 and PAALA-12 and gives support to interpreting the former as arranged like in phase B. On the other hand, the structure of crystallized PAALA-8 has certain resemblances with the structure present in phase A. Such a structure may be described as an assembly of main chain layers with side chains filling the interlayer space although no independent paraffinic crystal phase is created in this case. If the 1.99 nm helical repeat found for PAALA-8 is assumed to be shared by higher members, the interchain distance separating the chains within the layers in phase A of each polymer may be estimated on the basis of their respective L_0 and density data. As shown in Figure 11, a nearly constant value of 1.25 nm results from such calculations. This calculated interchain distance is close to the a_0 of the hexagonal form of poly(α-ethyl β-L-aspartate), indicating that about two methylenes must be spent in the bending of alkyl side groups protruding from the layer plane. It should be noted that an interchain distance of 1.16 nm would be obtained for PAALA-6 by these means if a layered structure were assumed for this polymer. Such deviation is outside experimental error and corroborates the interpretation of the structure of PAALA-6 as a roughly hexagonal packing of helices.

A fairly detailed description of phase A has been attained. The distinctive feature of this structure is the existence of interlayer paraffinic crystallites formed by intercalating side chains in opposite directions. Evidence provided by different methods indicates that side chains must be crystallized in a hexagonal arrangement. Although this is the type of packing usually adopted by alkyl side chains in comblike polymers, it contrasts with the rhombic lattice described for the case of poly(γ-alkyl α-L-glutamate)s.[12] Such divergence may be accounted for in terms of differences in side chain flexibility; the ethylene spacer in polyglutamates will enable the alkyl group to be accommodated in a more stable rhombic lattice. In this regard, it is interesting to note that the interchain distance in the hexagonal paraffinic lattice is very close to the fourth of the axial repeat of the 13/4 helix. Furthermore, a similar planar density is calculated for the alkyl groups in both the main chain layer and the 001 plane of the hexagonal crystallites. This allows the side chain to continue along the structure without significant spatial disruption.

To summarize, the structural transformations underlying transitions A−B and B−C are schematically represented in Figure 12. The molecular organization in phase B is envisaged to be substantially like that in phase A but with side chains in a liquid state. Furthermore, optical observations suggest that successive main chain layers should be slightly rotated so that a supramolecular helical structure is created. Such structural proximity between phases A and B accounts for the instantaneous reversibility displayed by the transition at T_1. Unfortunately, the information available on the structure of phase C is much more scarce. The large decrease in L_0 at T_2 implies that the layered structure has been abandoned; otherwise, the density should increase to near 50%, which seems to be completely unreasonable. Although at this stage the structure of

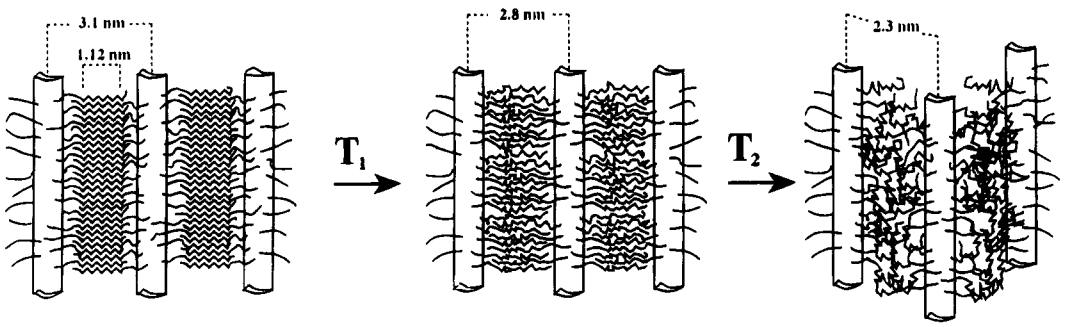

Figure 12. Schematic model illustrating the structural changes which take place in PAALA-n with $n \geq 12$ by effect of temperature. Distances are specified for the particular case of PAALA-18. Transition A → B at T_1: Paraffinic crystallites melt and the interlayer distance L_0 contracts from 3.1 to 2.8 nm. Transition B → C at T_2: The layered structure is abandoned and L_0 reduces to 2.3 nm, which is envisaged as the average distance separating the helices in phase C.

phase C can be only interpreted in a tentative manner, a nematic liquid crystal comprised of helices with an apparent diameter of 2.3–2.4 nm is thought to be a plausible model. Since the lateral alignment of the molecules would have been lost, recovering phase B upon cooling will not be straightforward, in agreement with experimental observations.

Concluding Remarks

Poly(α-*n*-alkyl β-L-aspartate)s are helical polyamides that closely follow the general pattern of behavior characteristic of poly(γ-*n*-alkyl α-L-glutamate)s. The combination of the rodlike character of the helical main chain with the more or less propensity of the side chain to crystallize the structure and thermal properties of both families of polymers.

The information afforded in this work together with that available in earlier studies on members containing short side chains provides a comprehensive picture of the structural and thermal behavior of the whole family of PAALA-*n*. Two groups of PAALA-*n* can be distinguished according to the manner in which they become organized in the solid state. PAALA-*n* with $n \leq 4$ crystallize into three-dimensional structures with side chains forming part of the main chain lattice. PAALA-*n* with $n \geq 12$ tend to organize into two-dimensional biphasic structures with main chain helices and alkyl side chains distributed into two separated domains. In the latter case, three structural phases, A, B, and C, differing essentially in the manner in which side chains are arranged have been identified as a function of temperature. In terms of mesomorphism, phase A may be regarded as structured in a sort of smectic-like phase with helices immobilized by the crystallized side chains. Phases B and C may be respectively envisaged as cholesteric and nematic arrangements with properties concomitant of lyotropic liquid crystals with the side chain playing the role of the solvent. Accordingly, thermal transitions in PAALA-*n* appear to follow the smectic–cholesteric–nematic sequence usually displayed by conventional thermotropic compounds. Further studies are needed to evaluate and characterize properly the thermotropic properties of these polyamides.

PAALA-*n* with side chains of intermediate size (n = 6 and 8) display a peculiar behavior reflecting the structural discontinuity existing between short and long side chain containing polymers. PAALA-8 exhibits a bimodal behavior; its structure in the uncrystallized state resembles that of phase B but the polymer may be crystallized in a three-dimensional lattice of the type adopted by short side chain containing members. PAALA-6 can neither crystallize nor organize in a biphasic structure.

Acknowledgment. This work has been supported by DGICYT (Grants PB-90-0597 and PB-93-0960) and by CICYT (Grant MAT-92-0707). F. L.-C. acknowledges financial assistance from the Venezuelan institutions Universidad de Los Andes and Fundayacucho. The authors are grateful to Dr. P. Lux from Bruker Spectrospin for his help with NMR experiments.

References and Notes

(1) Fernández-Santín, J. M.; Aymamí, J.; Rodríguez-Galán, A.; Muñoz-Guerra, S.; Subirana, J. A. *Nature (London)* **1984**, *311*, 53.
(2) Fernández-Santín, J. M.; Muñoz-Guerra, S.; Rodríguez-Galán, A.; Aymamí, J.; Lloveras, J.; Subirana, J. A. *Macromolecules* **1987**, *20*, 62.
(3) Muñoz-Guerra, S.; Fernández-Santín, J. M.; Alegre, C.; Subirana, J. A. *Macromolecules* **1989**, *22*, 1940.
(4) Montserrat, J. M.; Muñoz-Guerra, S.; Subirana, J. A. *Makromol. Chem., Macromol. Symp.* **1988**, *20/21*, 319.
(5) Prieto, A.; Pérez, R.; Subirana, J. A. *J. Appl. Phys.* **1989**, *66*, 803.
(6) López-Carrasquero, F.; Martínez de Ilarduya, A.; Muñoz-Guerra, S. *Polym. J.* **1994**, *26*, 694.
(7) López-Carrasquero, F.; Alemán, C.; García-Alvarez, M.; Martínez de Ilarduya, A.; Muñoz-Guerra, S. *Makromol. Chem. Phys.* **1995**, *196*, 253.
(8) López-Carrasquero, F.; García-Alvarez, M.; Muñoz-Guerra, S. *Polymer* **1994**, *35*, 4502.
(9) Bella, J.; Alemán, C.; Fernández-Santín, J. M.; Alegre, C.; Subirana, J. A. *Macromolecules* **1992**, *25*, 5225.
(10) López-Carrasquero, F.; Alemán, C.; Muñoz-Guerra, S. *Biopolymers*, in press.
(11) Platé, N. A.; Shibaev, V. P. *J. Polym. Sci., Macromol. Rev.* **1974**, *8*, 117.
(12) Watanabe, J.; Ono, H.; Uematsu, I.; Abe, A. *Macromolecules* **1985**, *18*, 2141.
(13) Iizuka, E.; Abe, K.; Hanabusa, K.; Shirai, H. In *Current Topics in Polymer Science*; Ottembrite, R. M., Ed.; Carl Hanser Verlag: Munich, 1987.
(14) Tsujita, Y.; Watanabe, T.; Takizawa, A.; Kinoshita, T. *Polymer* **1991**, *32*, 569.
(15) Iida, S.; Schaub, M.; Schulze, M.; Wegner, G. *Adv. Mater.* **1993**, *5*, 564.
(16) Romero-Colomer, F. J.; Gómez-Ribelles, J. L.; Barrales-Rienda, J. M. *Macromolecules* **1994**, *27*, 5004.
(17) Daly, W. H.; Poché, D.; Negulescu, I. *Prog. Polym. Sci.* **1994**, *19*, 79.
(18) Vives, J.; Rodríguez-Galán, A.; Muñoz-Guerra, S.; Sekiguchi, H. *Makromol. Chem.* **1989**, *10*, 13.
(19) García-Alvarez, M.; Rodríguez-Galán, A.; Muñoz-Guerra, S. *Makromol. Chem., Rapid Commun.* **1992**, *13*, 173.
(20) García-Alvarez, M.; López-Carrasquero, F.; Tort, E.; Rodríguez-Galán, A.; Muñoz-Guerra, S. *Synth. Commun.* **1994**, *24*, 745.
(21) Doty, P.; Bradbury, J. A.; Haltzer, A. M. *J. Am. Chem. Soc.* **1956**, *78*, 947.
(22) Romero Colomer, F. J.; Gómez-Ribelles, J. L.; Lloveras, J.; Muñoz-Guerra, S. *Polymer* **1991**, *32*, 1642.
(23) Ingwall, R. T.; Gilon, C.; Goodman, M. *J. Am. Chem. Soc.* **1975**, *97*, 4356.
(24) Turner-Jones, A. *Makromol. Chem.* **1964**, *71*, 1.
(25) Fraser, R. D. B. *J. Chem. Phys.* **1958**, *28*, 1113.
(26) Jordan, E. F.; Feldeisen, D. W.; Wrigley, A. N. *J. Polym. Sci., Part A-1* **1971**, *9*, 1875.
(27) Broadhurst, M. G. *J. Res. Natl. Bur. Stand.* **1962**, *66A*, 241.
(28) VanderHart, D. L. *J. Magn. Reson.* **1981**, *44*, 117.
(29) Yamanobe, T.; Tsukahara, T.; Komoto, T.; Watanabe, J.; Ando, I.; Uematsu, I.; Deguchi, K.; Fujito, T.; Imanari, M. *Macromolecules* **1988**, *21*, 48.
(30) Quintero-Arcaya, R. A.; Bovey, F A.; Fernández-Santín, J. M.; Subirana, J. A. *Macromolecules* **1989**, *22*, 2533.
(31) Okabe, T.; Yamanobe, T.; Komoto, T.; Watanabe, J.; Ando, I. *J. Mol. Struct.* **1989**, *213*, 213.

MA950101V